

Glucose Oxidase Adsorption on Sequential Adsorbed Polyelectrolyte Films Studied by Spectroscopic Techniques

Ferdinando Tristán, Araceli Solís, Gabriela Palestino, Csilla Gergely, Frédéric Cuisinier, and Elías Pérez

Citation: [AIP Conference Proceedings](#) **759**, 111 (2005); doi: 10.1063/1.1928164

View online: <http://dx.doi.org/10.1063/1.1928164>

View Table of Contents: <http://scitation.aip.org/content/aip/proceeding/aipcp/759?ver=pdfcov>

Published by the [AIP Publishing](#)

Articles you may be interested in

[Pressure Effect on the HelixCoil Transition of an AlaRich Peptide in Aqueous Solution: A FT IR Spectroscopic Study](#)

AIP Conf. Proc. **716**, 184 (2004); 10.1063/1.1796611

[Generalized 2D infrared spectroscopic study on protein structure of spider's thread](#)

AIP Conf. Proc. **503**, 287 (2000); 10.1063/1.1302879

[Effect of sucrose on the thermal denaturation of a protein: An FTIR spectroscopic study of a monoclonal antibody](#)

AIP Conf. Proc. **430**, 332 (1998); 10.1063/1.55793

[Synthesis and FT-IR study of Ln-Glucose-Pyridine complexes](#)

AIP Conf. Proc. **430**, 324 (1998); 10.1063/1.55791

[Vesicles containing ion channels on crystalline surfaces—An FTIR and surface enhanced FTIR spectroscopic study](#)

AIP Conf. Proc. **430**, 594 (1998); 10.1063/1.55732

Glucose Oxidase Adsorption on Sequential Adsorbed Polyelectrolyte Films Studied by Spectroscopic Techniques

Ferdinando Tristán^a, Araceli Solís^b, Gabriela Palestino^b, Csilla Gergely^c,
Frédéric Cuisinier^c, and Elías Pérez^{d,*}

^aCentro de Investigación y Estudios de Posgrado, ^bFacultad de Ciencias Químicas and ^dInstituto de Física Universidad Autónoma de San Luis Potosí, Álvaro Obregón 64, 78000 SLP, México and ^cINSERM U 595, Federation de Recherche Odontologiques, Université Louis Pasteur, 11 rue Humann, 67085 Strasbourg Cedex, France

Abstract. The adsorption of Glucose Oxidase (GOX) on layers of poly(allylamine hydrochloride) (PAH) and poly(acrylic acid) (PAA) deposited on Sequentially Adsorbed Polyelectrolyte Films (SAPFs) were studied by three different spectroscopic techniques. These techniques are: Optical Wave Light Spectroscopy (OWLS) to measure surface density; Fluorescence Resonance Energy Transfer (FRET) to verify the adsorption of GOX on the surface; and Fourier Transform Infrared Spectroscopy in Attenuated Total Reflection mode (FTIR-HATR) to inspect local structure of polyelectrolytes and GOX. Two positive and two negative polyelectrolytes are used: Cationic poly(ethyleneimine) (PEI) and poly(allylamine hydrochloride) (PAH) and anionic poly(sodium 4-styrene sulfonate) (PSS) and poly(acrylic acid) (PAA). These spectroscopic techniques do not require any labeling for GOX or SAPFs, specifically GOX and PSS are naturally fluorescent and are used as a couple donor-acceptor for the FRET technique. The SAPFs are formed by a (PEI)-(PSS/PAH)₂ film followed by (PAA/PAH)_n bilayers. GOX is finally deposited on top of SAPFs at different values of n (n=1..5). Our results show that GOX is adsorbed on positive ended SAPFs forming a monolayer. Contrary, GOX adsorption is not observed on negative ended film polyelectrolyte. GOX stability was tested adding a positive and a negative polyelectrolyte after GOX adsorption. Protein is partially removed by PAH and PAA, with lesser force by PAA.

INTRODUCTION

Sequentially adsorbed polyelectrolyte films (SAPFs) formed by alternated adsorption of polycations and polyanions in aqueous solution on a charged surface is a well known method to build multicomponent films on solid supports with a high degree of control on the film architecture and thickness [1]. Specific compounds are incorporated onto (or into) the films during the formation by replacing one polyelectrolyte of the same charge [2]. Biological compounds that are soluble and ionized could be directly incorporated in the SAPFs. Proteins adsorption and their incorporation in these films is matter of special interest because they can produce self-organized structures with potential biological applications [3-11]. Enzymes can be

* Corresponding author. Phone (52) 444 - 8 26 23 63. Email: elias@ifisica.uaslp.mx (E. Pérez).

used to design high specific biosensors [3, 4, 5] and proteins can be used as an intermediate agent between polyelectrolytes and cells [6].

Pioneering work with positive and negative proteins [7, 8] (at a given pH) showed that the adsorption of the water-soluble proteins onto and into the SAPFs was possible. A recent work has showed that proteins can be adsorbed on both positive and negative ending films [9]. This behavior was firstly observed for the Human Serum Albumin (HSA) [10]. HSA, a negative protein at pH 7.4, is adsorbed as monolayer on a negative polyelectrolyte or as multilayers on a positive polyelectrolyte. In both cases the adsorption process depends on internal and surface structure of SAPFs and on orientation and charge distribution of the protein. Two models related to these mechanisms are proposed to explain multilayers of HSA on the positive surface: i) multilayers on positive surface are formed by oriented HSA, with the positive region pointing toward the solution, ii) positive polyelectrolyte could emerge of the film forming complexes with proteins on the surface making possible formation of protein multilayers[10]. Experimental evidence of the protein diffusion on the surface seems to support the first model [11]

Some concepts are associated in these models: the molecular interdiffusion of polyelectrolyte in the film and the charge distribution and orientation of the protein when it is adsorbed onto the polyelectrolyte film. The first one depends on internal and surface structure of the SAPFs. Polyelectrolyte interpenetration (or interdigitation) between neighboring polyelectrolyte layers was determined by Neutron and X-ray Reflectivity experiments for two strong polyelectrolytes poly(sodium 4-styrene sulfonate) (PSS) and poly(allylamine hydrochloride) (PAH) showing that multilayer structure is maintained [12, 13]. Confocal laser scanning microscopy shows that polyelectrolyte interdiffusion is more marked for weak polyelectrolytes like poly(L-lysine) and hyaluronic acid (HA). Fluorescent-labeled PLL can diffuse into the SAPFs film even at a macroscopic scale [14]. The interdiffusion between positive and negative polyelectrolytes is also manifested in the thickness growth; strong polyelectrolytes show a linear growth with the number of layers, while the weak ones present an exponential behavior [15]. Polyelectrolyte interdiffusion is also revealed on the surface structure of SAPFs, where a granular structure is observed. Grains on the surface are associated with polyelectrolyte complexes [16, 17]. These surface complexes may produce positive sites on a net negatively charged surface explaining adsorption of negatively charged protein.

Charge distribution and protein orientation on SAPFs surface are difficult to determine [18]. Proteins are ampholyte molecules and their internal charge distribution depends on environmental conditions (pH, ion strength). Although, protein adsorption has been recognized to be mainly driven by electrostatic forces [7, 10] protein adsorption depends on the structure of polyelectrolyte films and charge distribution of the protein.

In this work, we studied GOX adsorption on the SAPFs with three complementary spectroscopic techniques to get pertinent information about the protein adsorption. These techniques are: Optical Wave Light Spectroscopy (OWLS) to measure SAPF thickness and adsorbed protein amounts; Fluorescence Resonance Energy Transfer (FRET) to verify the irreversible adsorption and the diffusion of GOX into the SAPFs and Fourier Transform Infrared Spectroscopy in Attenuated Total Reflectance (FTIR-

HATR) mode to inspect local environment of polyelectrolyte and GOX. These techniques have already been used for SAPFs. OWLS is used to find out thickness and relative refraction index of the film during multilayer build up [19] and FTIR-HATR have been used to study water presence [20], ion permeability [21] and the oxide-reduction process of the Os(II)/Os(III) [22]. Protein structure has been also studied by FTIR-HATR observing the bands corresponding to amide I and amide II [23, 24]. FRET has been used to determine energy transfer between poly(p-phenylene vinylene) (PPV) and labeled PAH [25], and interpenetration between PPV and anionically derivated poly(p-phenylene) (-PPP) [26]. Local energy transfer has been also observed directly by the scan probe microscope in a system formed by labeling PPV and PAH [27] In the present work the system PAA/PAH is used as a spacer to separate PSS layers, which is the fluorescent acceptor, from the GOX layer, which is the fluorescent donor in our FRET experiments. It fact, given the resonance condition between GOX and PSS no labeling is necessary for FRET experiments.

GOX is a protein that has been extensively studied in doped polyelectrolyte films using its electrochemistry properties [3,4,5]. The spectroscopic techniques presented here do not require that GOX should be electrically *wired* to an electrode surface [3] and they are able to give us information about adsorption, stability and charge distribution of this protein.

MATERIALS AND METHODS

Cationic poly(ethyleneimine) (PEI) and anionic poly(sodium 4-styrene sulfonate) (PSS) (Both from Acros, USA), cationic poly(allylamine hydrochloride) (PAH) (Alfa-Aesar, USA) and anionic poly(acrylic acid) (Aldrich, USA), all with $M_w \sim 7 \times 10^4$, and glucose oxidase (GOX) type VII-S ($M_w = 16 \times 10^4$) from *Aspergillus niger* (Sigma, France) is used. Polyelectrolytes and protein are dissolved in Mes-Tris buffer prepared with 2-(N-morpholino)ethanesulfonic acid (MES) at 25 mM, Tris(hydroxymethyl)aminomethane (TRIS) buffer at 25 mM and NaCl at 100 mM (all from Sigma, France). The buffer is adjusted to pH 6.8 with a 0.1 M HCl solution. It is used for OWLS and FRET experiments and simple saline water at 100 mM of NaCl is used for FTIR-HATR experiments. For FRET and OWLS experiments polyelectrolyte concentrations are 1 mg/mL and GOX concentration is 200 μ g/mL. Polyelectrolyte and GOX concentration are 25 mg/mL and 2.5 mg/mL, respectively. Aqueous solutions are prepared using ultra pure water (Milli Q-Plus system, Millipore). It has to be noticed that all the solutions mentioned above had the same ionic strength. In all the SAPFs reported here, the first layer is formed by PEI. After this first layer, we deposit two bilayers formed by PSS and PAH and denoted by (PSS/PAH)₂. They are followed by several bilayers made with (PAH/PAA)_n ($n = 1 \dots 5$) and we deposit the protein on the last bilayer to finalize this procedure.

The OWLS technique works with TE and TM waves of a laser that are coupled into a planar waveguide of high refraction index ($n_f \sim 1.77$) through an input grating coupler[28]. This occurs only at certain values of the incident angle where the beams are diffracted by the grating coupler. The coupling angles are related to two effective refraction indexes: NTE and NTM, one for the TE mode and the other for the TM

mode. A polyelectrolyte or protein adsorbed on the planar waveguide perturbs the TE and TM modes. This increases NTE and NTM values. From these changes we can obtain the film thickness and refractive index of the layer of the polyelectrolyte and GOX in an *in situ* method. Experiments were carried out on a home-build experimental set up [19] with a 5 mW He-Ne laser and $\text{Si}_{0.8}\text{Ti}_{0.2}\text{O}_2$ waveguides (Microvacuum, Hungary). The wave guide is first cleaned by using a 10 mM SDS solution followed by a 0.1 N HCl solution for 15 min each in a boiling water bath. Buffer is flushed through the cell at a constant flow rate (10 ml/hour) with a syringe pusher (Bioblock Scientific, France) until equilibrium is reached (less than 10^{-5} variation on absolute values of NTE and NTM). After a stable baseline is obtained the buildup of the polyelectrolyte multilayer film is performed as follows: The buffer flow is stopped and 100 μl of the PEI solution is directly injected in the cell through the injection port. NTE and NTM values increase and reach a plateau after about 20 min. When a stable adsorption signal is obtained, the buffer flow is restarted for about 15 min to rinse the excess polyelectrolyte from the cell. We continue then with the alternative adsorption of negatively charged PSS (or PAA) and positively charged PAH. Thus the initial film and the PAA/PAH layers are progressively deposited and the GOX layer is finally adsorbed. NTE and NTM are followed during the polyelectrolyte and the GOX injections; surface density is calculated from these data [19].

FRET technique is based on the fluorescent energy transfer that occurs from donor to acceptor molecules, which must be in a close proximity [29]. A condition for this technique is that the emission spectrum of the donor overlaps the excitation spectrum of the acceptor [30]. The efficiency of energy transfer between two assemblies of molecules is a function of the separation between the donor and acceptor molecules [31].

Fluorescence resonance energy transfer measurements were carried out in a commercial lifetime spectrometer (C-700 TimeMaster PTI, Canada). This equipment uses a chromatic light that is produced by a 75 Watts xenon arc lamp, and two monochromators make the selection of the excitation and emission wavelength. A photon-counting photomultiplier measures the fluorescence intensity. Measurements are made at 90° orienting the support of the SAPFs at maximum detection.

The only two compounds used in our studied system have fluorescent properties: the protein (GOX) and the anionic polyelectrolyte PSS. PSS has a fluorescent group whereas the GOX has three: phenylalanine, tyrosine and tryptophan in a total weight proportion of 3.89%, 6.63% and 2.67%, respectively. [32] In this work, an effective fluorescent spectrum is considered to be a consequence of these three groups. SAPFs are prepared on a negative glass surface (Thuet B., France). The glass surface is $20 \times 10 \text{ mm}^2$. This glass surface is cleaned using the same procedure described above for wave guide plates. SAPFs are formed by following an *in situ* procedure inside of one flow cell. The flow cell consists of one quartz cell, a syringe which allows the introduction of liquid solutions into the cell, and two hoses. One of them is connected to the syringe by one side and is connected to the quartz cell by the other side. The second hose is also connected to the cell, but the other side goes to one container. This hose is used to drain the liquid solution from the cell. The procedure to prepare multilayer films is the following: at the beginning, we filled the cell and hoses with

buffer solution. The PEI solution is injected into the quartz cell. The cationic polyelectrolyte solution replaces the buffer solution that is initially in the cell. We left 5 ml inside the syringe, and we waited for 20 minutes until the PEI layer was deposited on the glass surface. After the 20 minutes, we introduce 70 ml of the buffer solution into the cell to wash the surface and remove any polyelectrolyte chains that are not attached to the surface. Then, all the steps mentioned above are repeated again using the anionic polyelectrolyte and we continue repeating this procedure alternating the cationic and anionic polyelectrolytes until the SAPFs are finished. The last layer deposited on this system is the GOX layer, obtaining PEI-(PSS/PAH)₂-(PAA/PAH)_n-GOX structures (n = 1 to 5). Samples are put in the sample holder for the fluorescence equipment, and first measures are done after approximately 20 minutes following the film preparation.

The FTIR experiments are performed in the Perkin Elmer 11600(USA) IR equipment coupled to a Horizontal Attenuated Total Reflectance cell (HATR). For FTIR measurement Mes-Tris buffer is avoided because it introduces some undesired IR bands in the polyelectrolyte and protein spectra. A simple saline solution is prepared for these experiments: 100 mM NaCl. The polyelectrolyte multilayer film is formed directly over the surface of the cell, on Zinc Selenide Crystal (Perkin Elmer, USA) with a surface of 5.2 X 2.0 cm². The polyelectrolyte solutions are deposited using a Pasteur pipette to get a thin liquid film over the crystal. We waited for 20 minutes until the polyelectrolyte is deposited onto the surface. Then the polyelectrolyte solution film is removed using another pasteur pipette and we applied a drying process by pumping air directly above the ZnSe crystal for 5 more minutes. The drying process is very important because the water signal superposes on the amine signal avoiding a correct detection. This procedure is repeated several times alternating the anionic polyelectrolyte and the cationic polyelectrolyte until we get the multilayer film over the ZnSe surface. Finally, over the polyelectrolyte film the protein (GOX) is deposited in the same way that each polyelectrolyte.

RESULTS AND DISCUSSION

The SAPFs formation and the GOX adsorption are first analyzed by OWLS. The results are shown in Fig. 1. The first five points correspond to the initial film: PEI-(PSS/PAH)₂. This film is formed by two highly ionizable polyelectrolytes, it is fluorescent because of the presence of PSS. The film formed by PEI-(PSS/PAH)₂ has a linear thickness growth behavior as reported before indicating a compact and layered structure.³³

After this initial film, all the remaining points correspond to polyelectrolyte injections used to get (PAA/PAH)_n bilayers. The (PAA/PAH)_n bilayers have an exponential behavior as n grows, indicating a diffusive exchange process among PAA and PAH molecules during the bilayer construction [15]. This change of regime from linear to exponential is due to the replacement of a strong polyelectrolyte (PSS) by a weak polyelectrolyte (PAA). Protein will then be deposited on the SAPFs where interdiffusion between polyelectrolytes occurs.

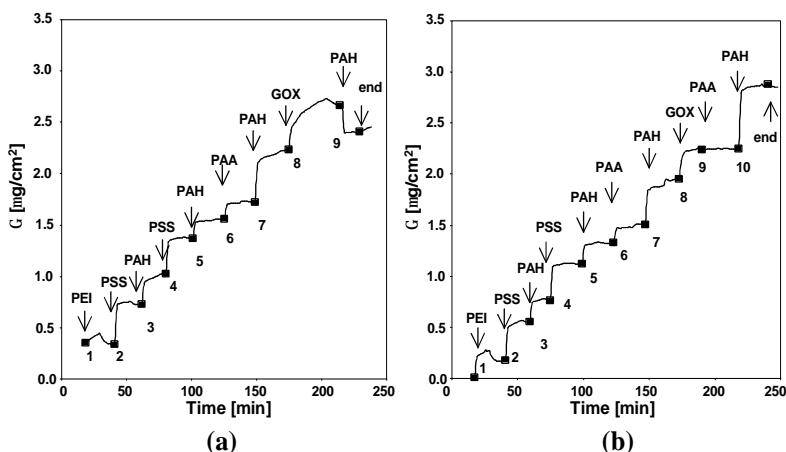


FIGURE 1. Surface density (Γ) for a) PEI-(PSS/PAH)₂-(PAA/PAH)₁-GOX-PAH and b) PEI-(PSS/PAH)₂-(PAA/PAH)₁-GOX-(PAA/PAH) by OWLS.

The formation of the SAPFs is followed using the surface density (Γ). In Figs. 1(a) and 1(b), the numbers under the curve indicate the injection of a polyelectrolyte. We started film formation with the initial film shown by the points: 1-5, then a PAA-PAH bilayer is formed (points: 6-7). The film follows the sequence denoted by PEI-(PSS/PAH)₂-(PAA/PAH)₁. GOX is deposited onto the positive PAH endlayer (point 8). In Figure 1(a), surface density (Γ) after rinsing which is a function of the thickness is calculated to be: $0.46 \pm 0.1 \mu\text{g}/\text{cm}^2$. It can be transformed to an average surface coverage percentage (q) using the formula: $q = \left(\frac{G}{M}\right) N_A A_p$; where M is the protein

molecular weight; N_A is the Avogadro's number and A_p is the projected dimensions of the protein molecule on the surface.⁹ The dimensions of one GOX molecule are $60 \text{ \AA} \times 52 \text{ \AA} \times 77 \text{ \AA}$ [34], so the average surface coverage is $q = 61 \pm 13 \%$, which indicates that negative GOX is adsorbed onto positive surface like a monolayer. This value is close to that predicted by the theory of random sequential adsorption (RSA): 54.7 %. [35]

In order to continue the SAPF formation, PAH is then injected on the GOX ended film (Fig. 1(a): point 9). The film surface density decreases abruptly reaching a value of $0.22 \pm 0.05 \mu\text{g}/\text{cm}^2$. This is showing that the GOX is partially removed by the polyelectrolyte and the charge on the GOX layer is not enough to allow the deposition of a PAH layer. The evidence indicates a weak interaction GOX-SAPFs compared with GOX-PAH interaction near the surface.

The behavior of the adsorbed GOX on the positive ended film when PAA is injected is shown in Fig. 1b, where surface density is again plotted versus time. The first five points represent the initial film formation. After the first PAA/PAH bilayer GOX is injected (Fig. 1(b): point 8). At point 9 PAA is injected and surface density is constant until the injection of PAH (point 10). The Γ value in this plateau is $0.33 \pm 0.17 \mu\text{g}/\text{cm}^2$. Which yields: $q = 44.3 \pm 22.8 \%$, indicating that protein is adsorbed in a monolayer. The last q value has only one meaning in the range from GOX to PAA

injections. After the PAA injection (point 9), we can not calculate protein surface coverage percentage because we do not know exactly the quantity of protein that remains on the surface. Injection of PAH (point 10) also reveals the possibility to continue the SAPF formation. There are evident differences between this case and the previous one. The conditions in which GOX is adsorbed are revealed by FRET and FTIR-HATR experiments shown below.

Similar experiments are carried out to observe GOX adsorption onto negative PAA polyelectrolyte but GOX adsorption is not observed at the present experimental conditions. This is contrary to other studies where proteins are adsorbed on surfaces with the same electrical charge. [7, 10] Therefore, GOX has an effective behavior of a negatively charged molecule. This study is therefore focused to GOX adsorption on the positive ended SAPFs and this is the only situation considered in the following two techniques.

FRET can give us additional information about GOX adsorption on SAPFs. Emission and excitation spectra are obtained for both PSS and GOX in solution (Fig. 2(a)). GOX emission and PSS excitation spectra are overlapped; therefore FRET can be used because the main condition is satisfied. [30] The GOX and PSS are donor and acceptor molecules, respectively. The peaks of these spectra are the following: GOX is excited at 284 nm and emission is obtained at 332 nm. On the other hand, PSS is excited at 322 nm and emission is obtained at 380 nm.

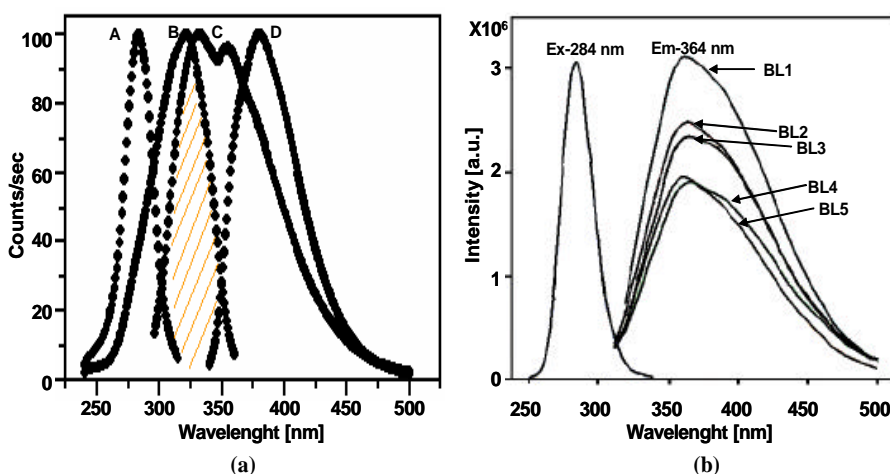


Figure 2. a) Fluorescence spectra for: A) GOX (Ex-284), B) PSS (Ex-322), C) GOX (Em-332) and D) PSS (Em-380) in solution. b) PSS emission spectra obtained by FRET in PEI-(PSS/PAH)₂-(PAA/PAH)_n films where n=1...5.

FRET experiments consist in exciting the donor molecule and observing the emission from the acceptor molecule: exciting GOX at 284 nm and recording the emission spectrum of PSS in the range from 250 nm to 500 nm. We made SAPFs having a different number of PAA/PAH bilayers between the PEI-(PSS/PAH)₂ fluorescent film and GOX placed on the top of the SAPFs. Results are shown in Fig. 2(b). As we show there, spectra obtained in solution are a good approximation of the spectra obtained when GOX and PSS are adsorbed onto the SAPFs. Measuring the

intensity of the emission of acceptor molecules, we notice that intensity decreases when the number of (PAA/PAH) bilayers increases.

This is a consequence of the resonance energy transfer from GOX to PSS. Maximum emission intensity is obtained when there is only one (PAA/PAH) (Fig. 2b: BL1) bilayer whereas emission intensity is minimum when there are 4 and 5 (PAA/PAH) bilayers (Fig. 2b: BL4, BL5). When we reached this point, the fluorescent molecules located in different layers (PSS and GOX) are far enough to avoid resonance energy transfer.

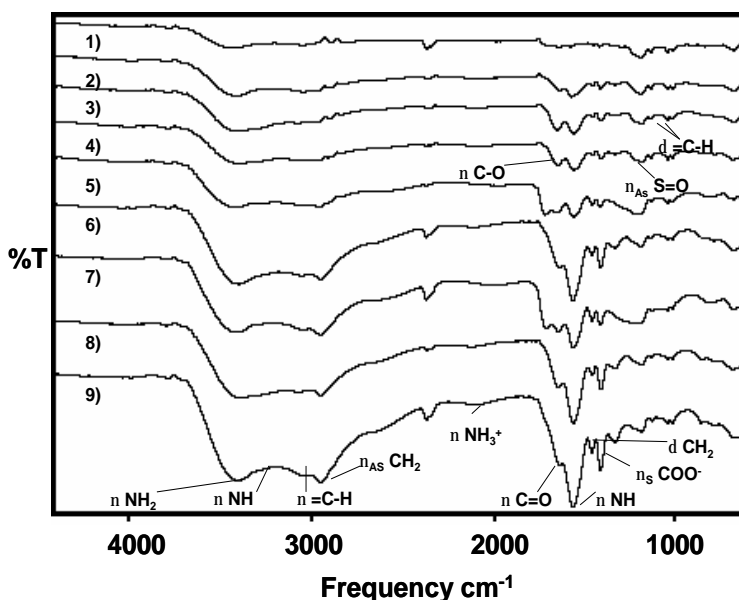


Figure 3 Multilayer buildup monitored by FTIR-HATR: (1PAA/2PAH)-3GOX-4PAH-(5PAA/6PAH)-7GOX-(8PAA/9PAH)

FTIR-HATR allows us to follow multilayer film formation and gives us structural information about each layer including GOX. The spectra obtained by this technique are shown in Fig. 3. The spectra are reported after the PEI-(PSS-PAH)₂ film. The curve 1 and 2 are obtained after the deposition of the first (PAA/PAH) bilayer. PAA has some characteristic adsorption band, especially due to the carboxylic acid groups (COOH). These bands are observed at 1704 cm^{-1} (C=O) and 1231 cm^{-1} (OC-OH). On the other hand, PAH has characteristic bands at 1546, 1404 and 1312 cm^{-1} that correspond to the $\text{(COO}^-\text{---}^+\text{NH}_3\text{)}$ and d(C-H) vibrations respectively. The increase showed by these bands while PAA and PAH are deposited is evidence enough to demonstrate that they are adsorbed on the multilayer. Polyelectrolyte backbone chains show characteristic bands due to the methylene groups (CH_2) at 2934 cm^{-1} , (C-H) and 1447 cm^{-1} d(C-H) . Strong modifications in the intensity and shape of the IR spectra are observed after the GOX deposition (curve 3) indicating that the protein is adsorbed on the multilayer. There are eight characteristic bands for GOX: free amine bonds (3414 and 3270 cm^{-1}); amide band I (1549 cm^{-1}); amide band II (1633 cm^{-1});

carboxylate bonds ($1549, 1405\text{ cm}^{-1}$); C-H aliphatic and protonated amine bands (overlapping in 2944 and 1458 cm^{-1}). We continue adding a PAH layer (curve 4) but the spectrum is slightly modified due to the GOX remotion from the surface. No adsorption of the PAH on the multilayer is identified. Later a PAA/PAH bilayer is added, and the modifications in the spectra around 1500 to 1750 cm^{-1} (curves 5 and 6) are showing the adsorption of both PAA and PAH on the multilayer. This zone shows two main bands corresponding to the amide group, free amine, also one band of the carboxylate and carboxyl groups present also one band in this zone. The IR spectrum taken before PAA deposition shows that the bands have an important intensity because some amine groups are free and they are not interacting with any specific group. After PAA deposition, intensity and shape of the bands are modified because the amine groups of PAH are now linked with the carboxylate groups of PAA and only a small fraction of protonated acid belonging to PAA is free, and these groups allow the adsorption of the PAH layer. However, when a GOX layer is added on the top of this multilayer the enzyme is not adsorbed and the spectrum is not modified (curve 7) remaining the same as the previous spectrum (curve 6). Finally a new PAA/PAH bilayer is added (curves 8 and 9). Again adsorption for both polyelectrolytes is confirmed due to the modifications in the same zone of the spectra that it was discussed before.

CONCLUSIONS

A general description of the GOX adsorption on the SAPFs is presented here using experimental results of three complementary spectroscopic techniques: Optical Wave Light Spectroscopy (OWLS), Fluorescence Resonance Energy Transfer (FRET) and Fourier Transform Infrared Spectroscopy in Attenuated Total Reflectance mode (FTIR-HATR). These techniques give complementary information based on the optical properties and molecular levels of polyelectrolytes and the GOX protein. The results show that GOX behaves as a negatively charged molecule (at the used pH): the protein is adsorbed on positive polyelectrolyte (PAH), but not on a negative polyelectrolyte (PAA). GOX is adsorbed on PAH forming a protein monolayer. This behavior is modulated by the film structure and charge distribution of the protein when it is adsorbed on the SAPFs. When PAH is injected over the protein, GOX is mostly removed from the polyelectrolyte film. This indicates a stronger interaction between the PAH and the GOX in the solution, more than the PAH and GOX in the film. This is probably due to the PAA-PAH complex that is formed on the film diminishing the positive surface charge from the PAH on the film. FTIR-HATR results are also showing an interesting behavior after the GOX removal from the multilayer. The multilayer buildup can continue only by PAA/PAH adsorption showing the positive nature of the last layer on the film. After a new bilayer, GOX can not be adsorbed again over a new PAH layer probably due to the experimental conditions used for this multilayer. Further work is required to understand this particular GOX behavior.

ACKNOWLEDGMENTS

The authors acknowledge financial support from the "Biomolecular Materials Project": CONACYT-Mexico (ER026) and Mexico-France Program: SEP-CONACYT-ANUIES-ECOS France (M01-S01). F. Tristán and A. Solís thank to CONACYT for their scholarships.

REFERENCES

1. G. Decher and J. B. Schlenoff, *Multilayer Thin Films: Sequential Assembly of Nanocomposite Materials*. N.Y. Wiley, 2003.
2. G. Decher, *Science* **277**, 1232 (1997).
3. E. J. Calvo, F. Battaglini, C. Danilowicz, A. Wolosiuk, M. Otero, *Faraday Discuss.* **116**, 47 (2000).
4. E. J. Calvo, A. Wolosiuk, *JACS* **124**, 8490 (2002).
5. E. J. Calvo, R. Etchenique, L. Pietrasanta, A. Wolosiuk, *Anal. Chem.* **73**, 1161 (2001).
6. P. Schaaf, J. C. Voegel, *Pathologie Biologie* **50** (3), 189 (2002).
7. Y. Lvov, K. Ariga, I. Ichinose, T. J. Kunitake, *Chem. Soc.* **117**, 6117 (1995).
8. F. Caruso, K. Niikura, D. N. Furlong, Y. Okahata, *Langmuir* **13**, 3427 (1997).
9. G. Ladam, P. Schaaf, F.J.G. Cuisinier, G. Decher, J.-C. Voegel, *Langmuir* **17**, 878 (2001).
10. G. Ladam, C. Gergely, B. Senger, G. Decher, J.C. Voegel, P. Schaaf, F.J.G. Cuisinier, *Biomacromolecules* **1**, 674 (2000).
11. L. Szyk, P. Schwinté, J. C. Voegel, P. Schaaf, B. Tinland, *J. Phys. Chem. B* **106**, 6049 (2002).
12. J. Schmitt, T. Grünwald, G. Decher, P. S. Perahan, K. Kjaer, M. Lösche, *Macromolecules* **26**, 7058 (1993).
13. M. Lösche, J. Schmitt, G. Decher, W. G. Bouwman, K. Kjaer, *Macromolecules* **31**, 8893 (1998).
14. C. Picart, J. Mutterer, L. Richert, Y. Luo, G. D. Prestwich, P. Schaaf, J.-C. Voegel, P. Lavalle, P. *PNAS* **20**, 12531 (2002).
15. Ph. Lavalle, C. Gergely, F.J.G. Cuisinier, G. Decher, P. Schaaf, J.-C. Voegel, C. Picart, *Macromolecules* **35**, 4458 (2002).
16. J.-L. Menchaca, B. Jachimska, F. Cuisinier, E. Pérez, *Colloids and Surfaces A* **222**, 185 (2003).
17. R. Messina, *Macromolecules* **37** (2), 621 (2004).
18. C. A. Haynes, W. Norde, *Colloids and Surfaces B*, **2**, 517 (1994).
19. C. Picart, G. Ladam, B. Senger, J.-C. Voegel, P. Schaaf, F. J. G. Cuisinier, C. Gergely, *J. Chem. Phys.* **115**, 1086 (2001).
20. T. Farhat, G. Yassin, S. T. Dubas, J. B. Schlenoff, *Langmuir* **15**, 6621 (1999).
21. J. J. Harris, M. L. Bruening, *Langmuir* **16**, 2006 (2000).
22. C. Bonazzola and E. J Calvo, *Langmuir* **19**, 5279 (2003).
23. P. Schwinté, J.-C Voegel, C. Picart, Y. Haikel, P. Schaaf, B. Szalontai, *J. Phys. Chem. B* **105**, 11906-11916 (2001).
24. F. Caruso, D. N. Furlong, K. Ariga, I. Ichinose, T. Kunitake, *Langmuir* **14**, 4559 (1998).
25. B. Richter, S. Kirtein, *J. Chem. Phys.* **111** (11), 5191 (1999).
26. J. Baur, M. F. Rubner, J. R. Reynolds, S. Kim, *Langmuir* **15**, 6460 (1999).
27. G. M. Lowman, N. Daoud, R. M. Case, P. J. Carson, S. K., Buratto, *Nano Lett.* **1**-12, 677 (2001).
28. K. Tiefenthaler, W. Lukosz, *J. Opt. Soc. Am. B* **6**, 209-220 (1989).
29. Th. Förster, *Ann. Phys. (Leipzig)* **2**, 55 (1948). *Discuss. Faraday Soc.* **27**, 7 (1959).
30. B. W. Van der Meer, G. Coker, S. Y. Simon-Chen *Resonance Energy Transfer: Theory and Data*; Ed.; Wiley-Vch: New York, 1991.
31. B. I. Berlman, *Energy Transfer Parameters of Aromatic Compounds*, Academic Press, New York, 1973.
32. Protein Data Bank: <http://www.rcsb.org>.
33. G. Decher, Y. Lvov, J. Schmitt, *Thin Solid Films* **244**, 772-777 (1994).
34. H. J. Hecht, H. M. Kalisz, J. Hendle, R. D. Schmid, D. Schomburg, *J. Mol. Biol.* **229**, 153 (1993).
35. Z. Adamczyk, *Adsorption of Particles: Theory*. Encyclopedia of Surface and Colloid Science. 2002, pp 499.